Metallurgical and Materials Transactions A 45 (2014) 4907-4915

White-etching matter in bearing steel
Part1: Controlled-cracking of 52100 steel

W. Solano-Alvarez[a], H. K. D. H. Bhadeshia[a]
[a]Materials Science and Metallurgy, University of Cambridge, U.K.

Abstract

Although most of the research performed in bearing steel metallurgy aims to prevent crack nucleation and propagation, some applications require the exact opposite in order to study the role that disconnected surfaces inside the bulk material play when load is applied, or when fluids entrapped in surface cracks propagate tensile stresses or exacerbate corrosion. Four heat treatments have been designed to create controlled arrays of crack types and distributions in a quenched and untempered steel normally used in the manufacture of bearings. The varieties of cracks studied include sparsely distributed martensite-plate cracks, fine grain boundary cracks, abundant martensite-plate cracks, and surface breaking cracks. The intention was to create samples which can then be subjected to appropriate mechanical testing so that phenomena such as the appearance of "white-etching areas" or "white-etching cracks", crack-lubricant interactions, or hydrogen trapping can be studied further.

Keywords: bearing steel, indentation cracks, cracked martensite, grain-boundary decohesion, surface cracks

1. Introduction

Bearings are subjected to complex and repeated contact loads, which induce damage that accumulates and ultimately leads to failure or removal from service when monitoring systems identify precursors to failure. However, it is not clear whether some of the damage that is detected in post-service examinations is the cause or consequence of failure. In order to gain confidence in the mechanisms of failure, it is necessary to be able to reproduce damage phenomena in controlled experiments, where the ambiguity of interpretation is reduced. There is a particular kind of microstructural damage in the form of regions of the structure, which appear white in etched metallographic samples, that is a cause of controversy in the context of failure mechanisms in large bearings used in wind turbines [1]. The hard regions of white-etching matter are sometimes identified with the cause of failure, and the mechanism by which this structure forms has been associated with diverse phenomena such as severe localised deformation, adiabatic shear, carbide dissolution, and low-temperature recrystallisation [1–4].

An alternative interpretation is that the process begins with the initiation of a microcrack [5], which then develops the white-etching matter by the rubbing together of the

crack surfaces, causing intense, localised mechanical deformation [4]. The design of better bearing steels depends on a clarification of these issues. For example, the idea that white-etching matter formation is the cause of failure would require different issues to be addressed, whereas if cracking precedes white-etching matter formation, then the problem can be mitigated by enhancing the resistance to cracking [5].

One way of establishing the mechanism is to subject samples, in which microscopic cracks are introduced deliberately, to rolling contact loading. Such experiments would reveal whether white-etching matter development in the pre-cracked samples occurs at the internal crack faces with greater vigour, than in specimens that do not contain cracks. They could also help establish whether damage development is a function of the orientation of the crack faces relative to the principal stresses during rolling contact loading. However, to conduct such experiments it is necessary to create populations of cracks which permit the steel to survive rolling contact loads for a significant number of cycles, sufficient to stimulate white-etching matter, but less than that required to cause gross fracture over the period of the test. The cracks that are relevant are classified as 'very short', typically 1-10 μm in length [6]. The purpose of the present work was, therefore, to design methods for creating such cracks, as a prelude to critical experiments that are reported in Part 2 [7].

The study of microscopic cracking in strong steels, including those used in the manufacture of bearings, has a significant history in the published literature. In high-carbon steels the martensite can crack when plates growing on different habit planes impinge [8–12]. The general consensus is that the austenite grain size (mean lineal intercept $\overline{L_\gamma}$), the amount of carbon in the martensite, and the transfer of stress between the martensite and austenite are important parameters in controlling crack formation [9, 12–14]. A large austenite grain size promotes martensite cracking, although it is reported that the quantity of cracking does not change much once $\overline{L_\gamma} \gtrsim 100$ μm [9]. This is consistent with the fact that the size of martensite plates scales with $\overline{L_\gamma}$, and once the austenite grain size becomes smaller than the stress transfer length of composite theory, it becomes difficult to transfer load onto the plates, thus reducing their tendency for cracking [12].

The susceptibility of martensite to brittle fracture naturally increases with its carbon concentration [13, 14] due to the well-known intense strengthening caused by the presence of carbon in interstitial solution in the otherwise body-centred cubic lattice of ferrite. There are secondary effects due to changes in martensite crystallography, which can alter the impingement angles between different variants [8]. Other forms of cracking that could be introduced deliberately include fracture at the γ-grain boundaries [15], often exacerbated by quenching stresses or impurity embrittlement. However, coarse grain boundary cracks can lead to premature failure under mechanical testing, before white-etching matter is formed.

In summary, the intention of the present work was, on the basis of the prior knowledge described above, to create a system of cracks which would be suitable for studying mainly the

white-etching matter evolution in bearing steels, but also secondary effects such as hydrogen trapping [16].

2. Experimental Methods

The material used in this study is a hot-rolled and spheroidised 52100 steel (table 1) manufactured by Ovako as a 60 mm diameter rod, from which cylindrical samples 120 mm long and 10 mm in diameter were machined for the purposes of heat treatment. The austenite grain size was determined using thermal etching [17] with a thermomechanical simulator Thermecmaster Z and cylindrical samples 12 mm long and 8 mm. The mean linear intercept $\overline{L_\gamma}$ was measured from optical micrographs of the thermally-etched samples, with sufficient measurements to ensure a standard error < 1%. These results were corroborated using image analysis software that computes the area of enclosed regions.

Table 1: Chemical composition, wt%, of the 52100 steel used.

C	Cr	Mn	Mo	Si	Ni	Al	P	S	Cu	Co	Ca	Ti
0.98	1.38	0.28	0.06	0.28	0.18	0.04	0.01	0.017	0.21	0.015	0.001	<0.001

The heat treatments designed to induce cracks were carried out using a box furnace, with the temperature monitored using K-type thermocouples spot-welded to the samples. The quenchants used were air, water, and GP460 oil at different temperatures. The volume of the oil used was approximately 10 l; the oil had a density at 15 °C of 904 kg m^{-3} and a viscosity index of 98 (ISO 2909). After oil quenching, samples were rinsed in water at ambient temperature.

Vickers hardness tests were carried out using a 30 kg load; the values reported correspond to the mean and standard error of ten indentations. Surface cracks were created through Vickers indents with a 130 kg load.

Optical microscopy on samples prepared to a 1 μm finish was conducted in both the etched (2% nital) and unetched conditions, in the latter case to ensure clarity in the detection of cracks.

3. Results and discussion

The initial spheroidised microstructure (fig. 1) has a hardness of 193±2 HV30 and consists of ferrite grains and cementite particles, the later ranging from 0.5 to 2 μm, consistent with reported data [18]. The size of the ferrite grains and cementite particles will determine the austenite grain size, as discussed in the following section, especially if the austenitisation conditions are not sufficient to dissolve the cementite [19].

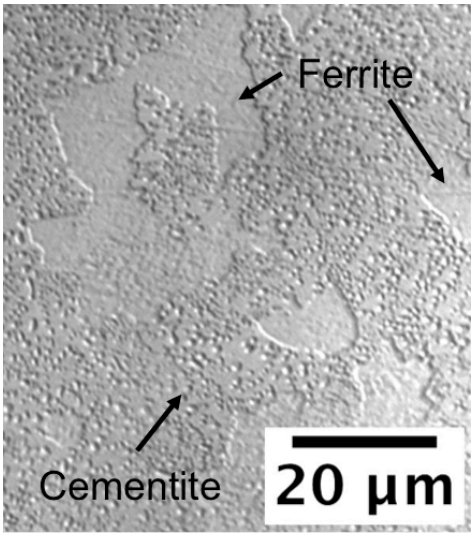

Figure 1: As-received 52100 steel in its spheroidised condition, consisting of a mixture of cementite particles and ferrite.

3.1. Prior austenite grain size determination

The austenite grain size was characterised in two ways (table 2): a mean lineal intercept determination is relevant because it is a fundamental measure of the surface per unit volume, and the second method involved image analysis to obtain a "grain diameter". In this second method, the software computes the area in pixels of enclosed regions and the measure is then translated into micrometres through a scale. By assuming a circular shape of grains, the diameter or grain size was computed. In both of cases, there is a potential uncertainty caused either by faint contrast or twins. The sizes obtained were within the ranges found in the literature of 40-60 µm after austenitisation at 1313 K (1040 °C) for 20 min [4].

Table 2: Average and standard deviation of prior austenite grain sizes for different analytical methods.

Method	Grain size for different austenitisation treatments	
	1223 K (950 °C), 10 min	1373 K (1100 °C), 10 min
Mean linear intercept	19±5 µm	49±33 µm
Grain diameter	16±9 µm	39±27 µm

The large standard deviations for T_γ=1373 K (1100 °C) is due to uneven grain growth between the centre and the edges of the sample, presumably caused by the short austenitisation times used of 10 min (fig. 2). Larger austenite grains permit longer martensite plates, which are more prone to cracking [8, 10, 12]. Therefore, the larger scatter of coarser grains in the 1373 K (1100 °C) sample should lead to an increased probability of microcracking, a fact that was exploited to design the extensive martensite plate cracking treatment described in section 3.3.

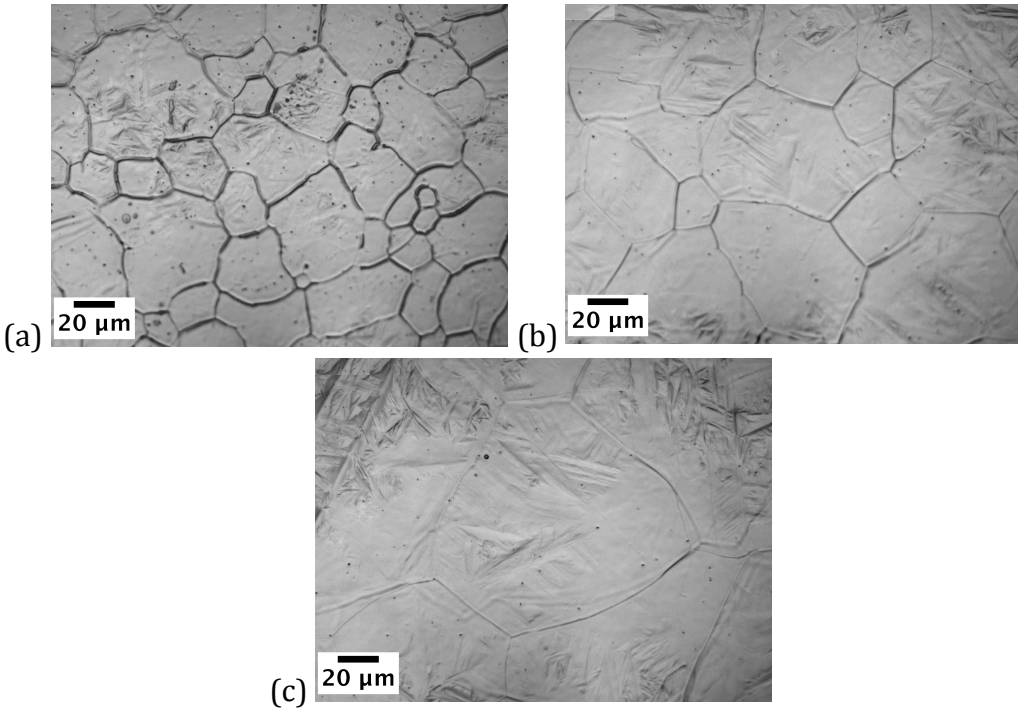

Figure 2: a) Prior austenite grain boundaries just below the surface of a sample austenitised at T_γ = 1373 K (1100 °C) for 10 min, b) 2 mm below the surface, and c) at the centre of the sample.

3.2. Production of infrequent fine-cracks

The length of martensite plates can be controlled via the austenite grain size. The severity of the quench, which influences the homogeneity of thermal stresses, can in turn be adjusted by using different cooling media, their temperatures, and levels of agitation. However, the influence of different levels of agitation was not investigated in this study. The initial experiments were performed with a set austenitisation time of t_γ=10 min and water as the quenchant. Since the first samples austenitised at T_γ=1373 K (1100 °C) displayed extensive grain boundary cracking, lower T_γ values and quenching into hotter water was pursued. The minimum T_γ used was 1113 K (840 °C), as this is the standard for 52100 steel bearings, and a treatment that leaves the most crack-free microstructure. For the sake of brevity, in subsequent discussion we use the notation 0000-00Q where the first four digits represent T_γ in Celsius, followed by the temperature of the quenching medium, which is identified by the letters W or O to represent water and oil respectively. The austenitisation time for these infrequent fine-crack treatments was always 10 min.

The least severe water-based heat-treatment, 840-92W, still led to profound grain boundary cracks, so the quenchant was changed to oil, for which the same procedure was followed except that the oil was kept at room temperature for safety reasons. Only by using T_γ=1173 K (900 °C) and quenching in oil at 295 K (22 °C) (900-22O), could the networks of coarse grain-boundary cracks be suppressed, although finer boundary cracks persisted, as illustrated in fig. 3a. Lower T_γ values were tested until only martensite-plate cracks were obtained for T_γ=1153 K (880 °C) (fig. 3b). However, cracks could not be detected once T_γ<1133 K (860 °C). Martensite plate cracks were scarce due to the short austenitisation

times used in this experiment that did not allow the austenite grains to coarsen much (see previous section). Martensite plate cracks can normally be distinguished from grain boundary fracture because they typically are only ~5 μm long with serrated contours. Nevertheless, confusion can arise from crack-like features like thin manganese sulphide inclusions or unevenly etched regions, avoided by observing uneteched samples.

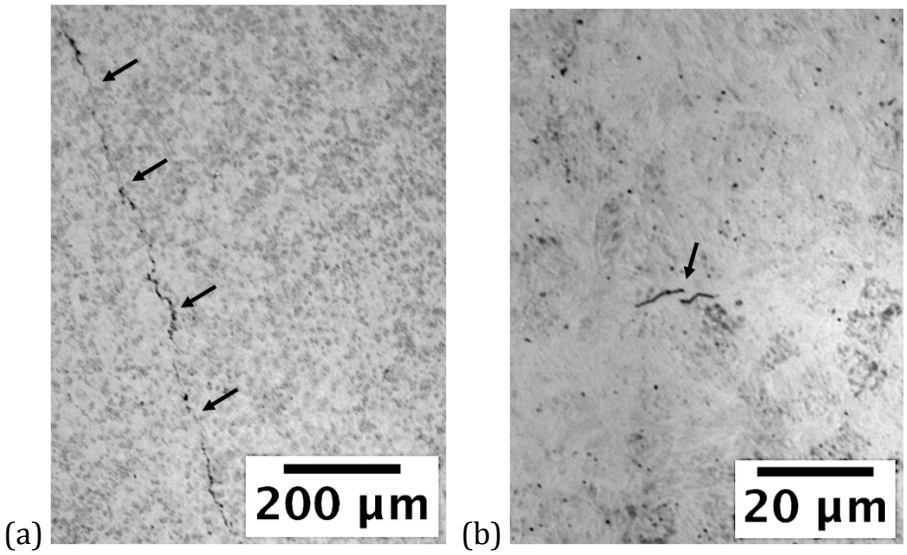

Figure 3: a) A fine grain boundary crack in sample 900-22O. b) Martensite plate cracks in sample 880-22O.

3.3. Extensive martensite plate cracking treatment

T_γ=1373 K (1100 °C) creates large austenite grains and hence, long and crack-prone martensite plates. Nonetheless, the large thermal stresses associated with the quenching from such high temperatures, even in oil, induce macroscopic grain boundary cracks. According to the continuous cooling transformation diagram of an alloy similar to 52100 steel (fig. 4), quenching can take about 60 s over the range of 1113 K (840 °C) to 473 K (200 °C) without the risk of forming pearlite (P) or bainite (α_b). Therefore, in order to maximise martensite plate cracking whilst avoiding boundary fracture due to thermal shock, samples were austenitised at the lowest temperature of the γ phase field for long times, but cooled in still air for close to 50 s, which reduced the temperature to around 923 K (650 °C), and finally quenched in oil at room temperature for 5 min before rinsing in water.

This treatment was first tested on a small thin sample 40 mm long, 8 mm wide, and 2 mm thick austenitised at 1313 K (1040 °C) for 30 min, cooled in air for 45 s, and quenched in oil at room temperature. The hardness achieved was 810 HV30 and many martensite plate cracks were obtained. However, to replicate this treatment for a rod sample, the austenitisation time was tripled to 90 min followed by cooling in air for ~55 s, and quenching in oil at room temperature, which created many martensite plate cracks in a sample with a hardness of 751 HV30 (fig. 5).

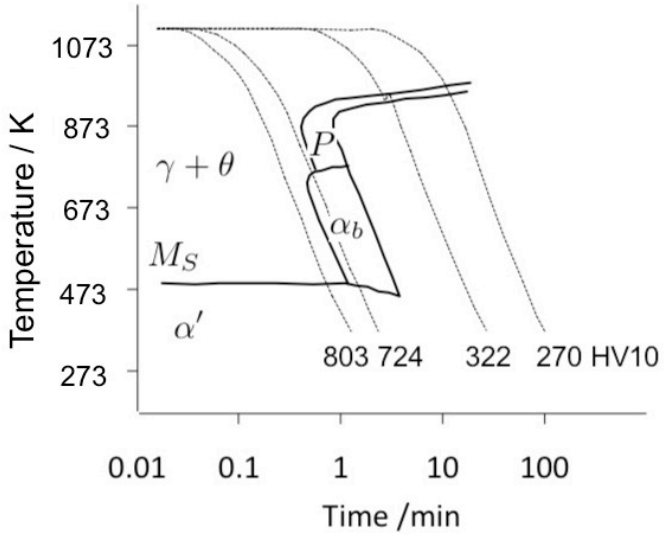

Figure 4: Continuous cooling transformation (CCT) diagram for 100Cr6 alloy:Fe-0.95 C-0.36 Mn-0.28 Si-1.84 Cr wt% showing: pearlite (P), bainite (α_b), martensite(α'), the martensite start temperature (M_s), and the austenite + cementite phase field ($\gamma + \theta$) [4] adapted from [20].

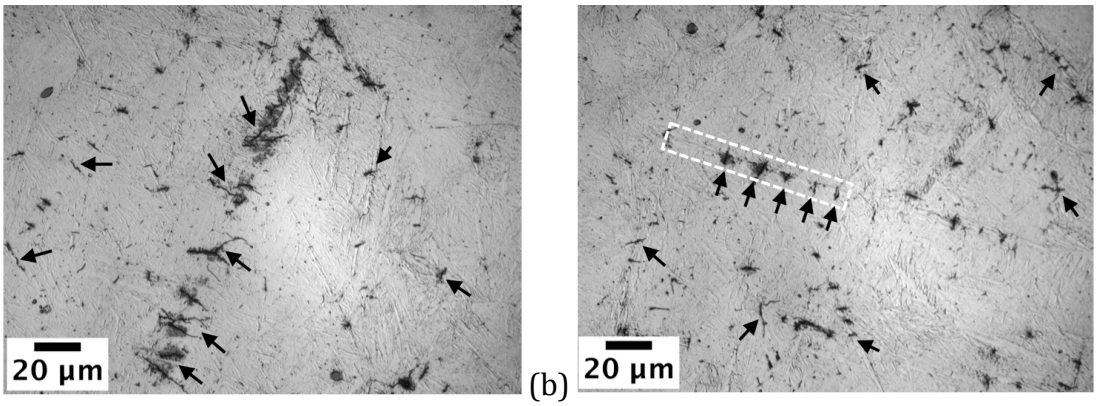

(a) (b)

Figure 5: Final extensive martensite plate cracking heat-treatment depicting a) large cracks in the centre of the sample and b) smaller cracks close to the free surface. Martensite plate cracks form as families of parallel cracks that cut across the plates, as shown in b) where the black arrows indicate the cracks and the white box, a martensite plate.

In order to replicate the martensite plate cracking treatment for a different alloy, the austenitisation temperature should be set so that undissolved cementite does not limit the growth of austenite grains and to dissolve sufficient carbon in the austenite to render the martensite plates brittle and prone to fracture. Based on the results obtained in this study, the austenitisation time should be adapted depending on the thickness of the sample so that the prior austenite grains are larger than ~40 µm. The chemical composition of the alloy is also important in defining the maximum time available for quenching to the martensite-start temperature; the quenching medium should minimise the quench stresses to avoid large quench-cracks. As mentioned previously, factors such as the type of quenchant, its temperature, level of agitation, volume, or even multiple quenching media need to be considered.

3.4. Inducing surface cracks

It is sometimes necessary to introduce microscopic surface-breaking cracks, for example, to study how the transmission of contact pressure to the crack front via the pulsating lubricant influences damage evolution [21]. Such cracks have in the past been achieved by indenting the bearing raceway so that the resulting stress concentration during rolling contact initiates the crack, but local surface upheavals cause particular distributions of stress during repeated rolling contact [22]. A new method was designed that avoids the upheavals, whereby an indentation is used to immediately induce some surface-breaking cracks, followed by grinding to smooth the surface while retaining the cracks.

Initial attempts involved indentation with 90 kN silica sand with a particle size of about 300 μm and a hardness of about 900 HV30 into as-received (193 HV30) and heat-treated samples (514 HV30). The indents, illustrated in fig. 6a, did not induce the desired cracks, presumably because of the relatively low hardness of the samples. Therefore, bending fatigue tests were carried out in an attempt to open up cracks at the indent tips on thin samples (40×8×2 mm), as illustrated in fig.6b, using a fixed displacement of 0.7 mm, at 5 Hz. Since these tests did not succeed in producing the desired cracks after a reasonable number of cycles (3×10^3), a different approach was adopted as described below.

(a) 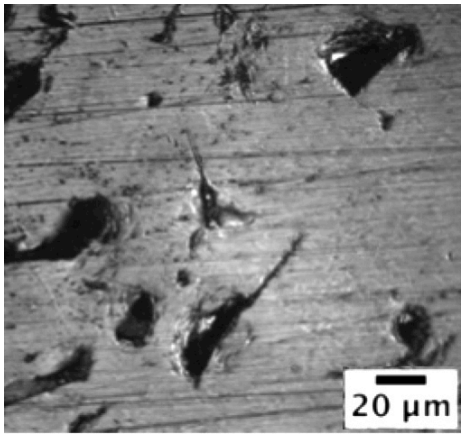

(b) 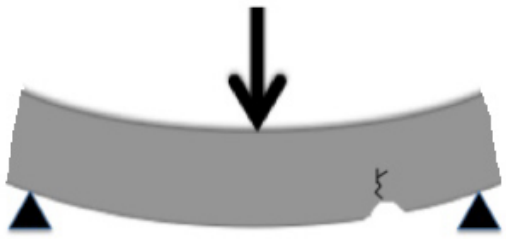

Figure 6: a) Indents created upon compression of silica sand against heat-treated sample and b) Schematic of bending fatigue testing to generate cracks at indentations.

Based on previous indentation cracking studies of embrittled steel [23], subsequent testing was performed using harder samples and Vickers indents with a load of 130 kg. Harder, more brittle samples, were sought by applying heat treatments that would completely dissolve the cementite, form martensite, but would not form any sort of quench crack. Since austenitising at 1313 K (1040 °C) for 20 min has been reported to dissolve all the cementite [24], a rod sample was austenitised at T_γ=1313 K (1040 °C) for 30 min, cooled in air for 50 s, and quenched in oil at room temperature, which created a martensitic grain boundary crack-free microstructure.

This treatment is similar to the one described above for extensive martensite plate cracking, but the shorter duration t_γ=30 min using a rod sample leads to a smaller $\overline{L_\gamma}$ and hence, a reduced tendency for microcracking. With a hardness of 764 HV30, the sample cracked upon hardness indentation even with a 30 kg load. Unlike the 130 kg load cracks, these 30 kg load cracks were fine so a procedure to extend them was developed. Just as incompressible lubricants fill surface cracks in bearings and propagate them by cyclically transmitting load to their tips, samples with fine surface cracks were introduced in a Stansted fluid power FPG2340 isostatic press, for tens of 60 s cycles at a pressure of 170 MPa whilst being submerged in a mixture of 10% Shell Dromus B oil and water. In order to ensure oil penetration into cracks prior to this cyclic pressurisation, the samples were placed in a GallenKamp1 kPa vacuum oven for 1.5 h at 313 K (40 °C), after which they were immediately submerged in the oil. As a result of the pressure cycles, the cracks became larger: 2.5±0.2 μm wide compared to original width of 1.3±0.09 μm (fig. 7).

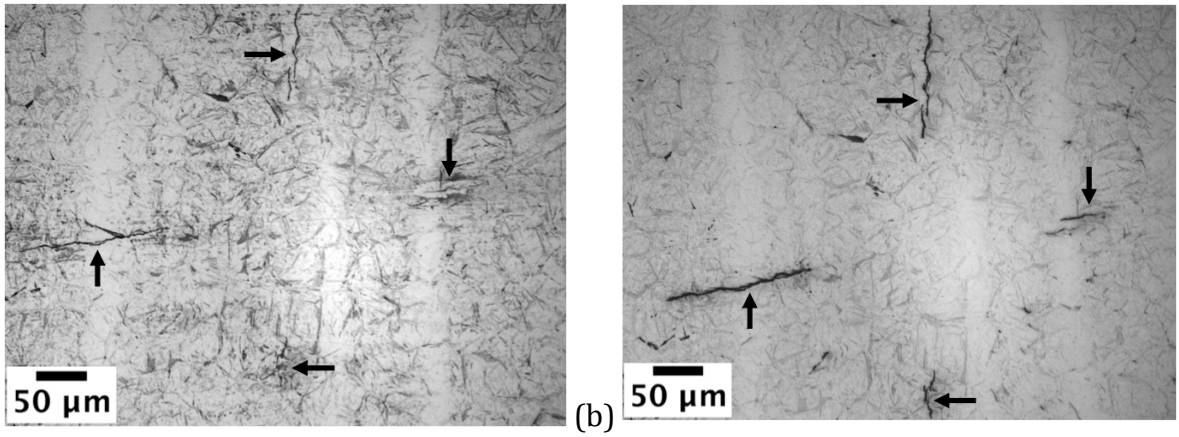

Figure 7: Indentation-induced cracks using a 30 kg load a) after the indent was barely ground away, and b) the same cracks after the isostatic pressure crack propagating treatment.

Another method used to amplify cracks was to submerge the previous sample in liquid nitrogen before further indentation. The cryogenic treatment stimulated the formation of additional martensite, resulting in an increase in hardness by 46 HV30 to 810 HV30. In order to study the influence of hardness on cracking, the depth of 30 and 130 kg indents with and without cryogenic treatment was calculated based on the geometry and size of the Vickers diamond indenter. The results are presented in table 3.

Table 3: Summary of indentation depths using different loads.

Vickers hardness indentation		
Load / kg	Cryogenic treatment	Calculated indent depth /μm
30	yes	51
	no	53
130	yes	107
	no	111

As expected, the increased hardness of the cryogenically treated samples gave rise to smaller, shallower indents and more extensive cracking. Although cracks created with both 30 and 130 kg loads remained after the indents were skimmed off by grinding, only the cracks created with a 130 kg load remained after the depth of grinding reached 250 μm, fig. 8, irrespective of liquid-nitrogen treatment. It is considered that in experiments involving real bearings, a depth of 250 μm would need to be removed from the surface after the final heat treatment in order to eliminate any decarburised layers, so surface cracks induced using the 130 kg load would be appropriate.

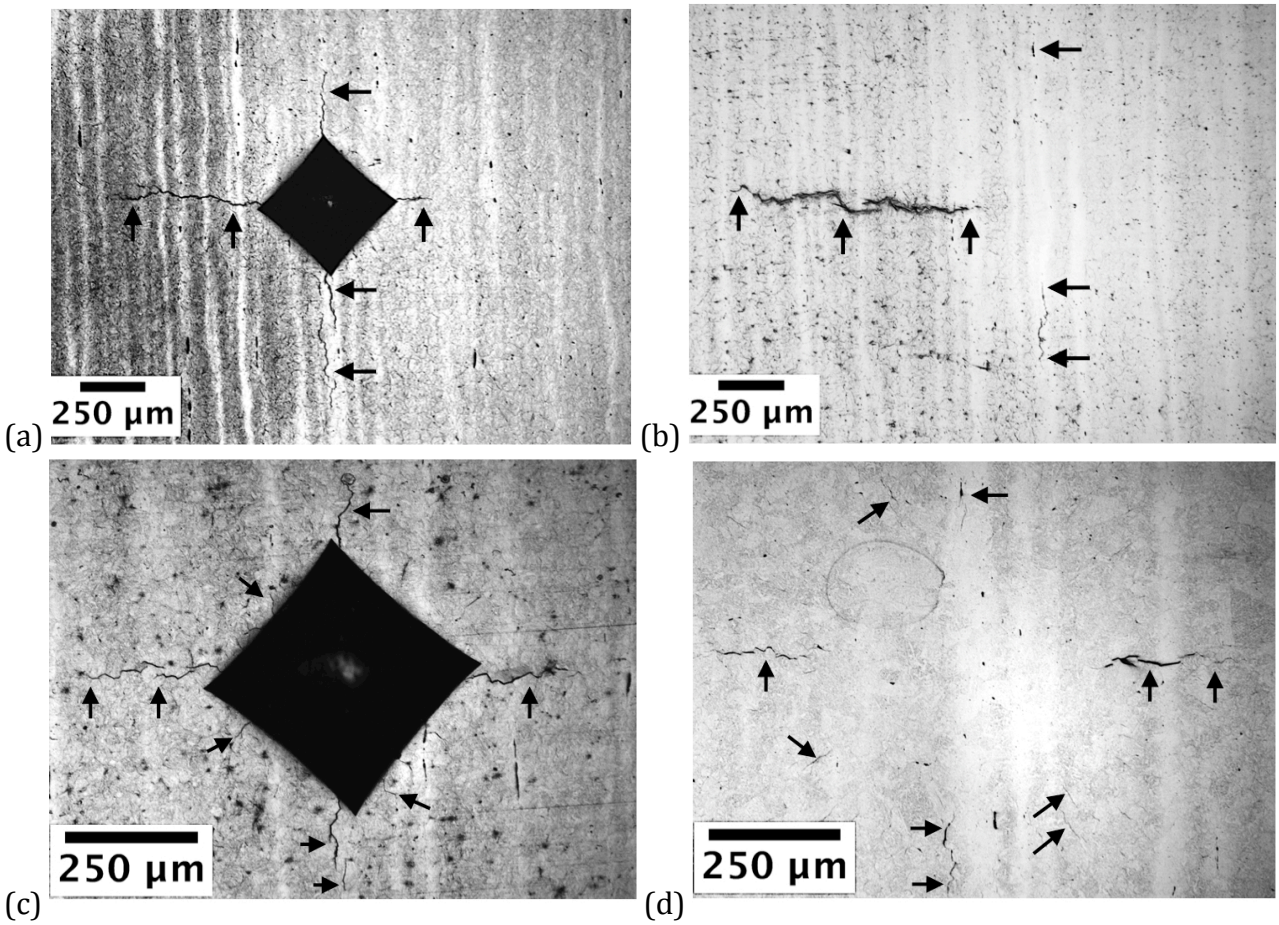

Figure 8: Hardness indentation using a 130 kg load showing a) indent-induced cracks on sample without liquid-nitrogen treatment, b) cracks remaining after 250 μm grinding, c) indent cracks on sample after liquid-nitrogen submersion, d) remaining cracks after 250 μm grinding.

Once cracks were proven to remain in the sample after deep grinding, this treatment was applied to a rod sample (120 mm long and 10 mm in diameter) austenitised at 1313 K (1040 °C) for 30 min, cooled in air for approximately 55 s to 906 K (633 °C), and quenched in oil at room temperature. The dimensions of the rod are such so it can be loaded in a Delta Research Corporation rod-ball rolling contact fatigue test rig. After heat treatment, the rod was indented ten times along its circumference. Optical microscopy images of this indent ring revealed an interesting range of crack morphologies, orientations, and sizes, different to what was observed in the flat samples, fig. 9.

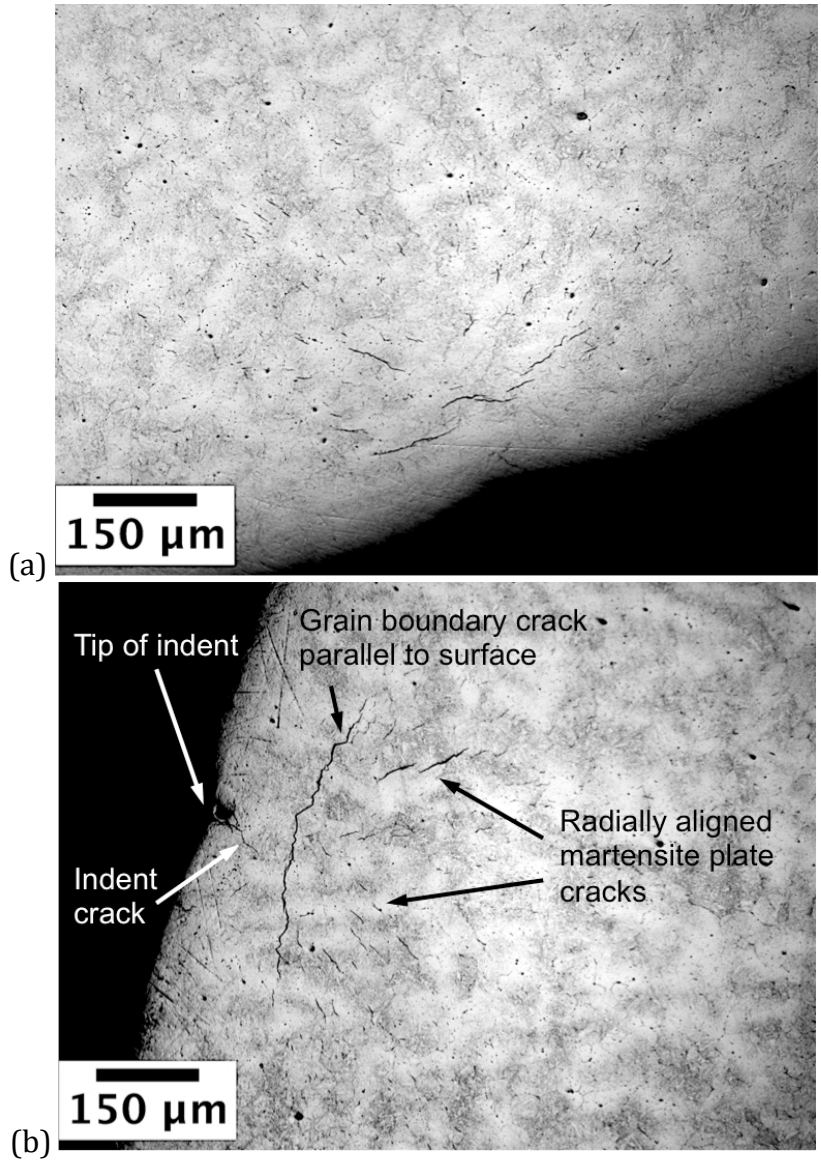

Figure 9: Radial cross section of rod sample showing two different indents and the different types and orientations of cracks produced.

At the bottom of every indent, a grain boundary crack normal to the surface reached a depth of approximately 100 µm. Instead, at a depth of 200 to 250 µm, long grain boundary cracks parallel to the sample surface could be observed. Finally, from a depth of 300 to 1000 µm, a family of martensite plate cracks all more or less radially aligned with the indent tip were apparent. Although no explanation for this phenomenon has been found, it is speculated that the cracks are due to the interaction of residual, radial tensile-stress at the surface of a quenched sample (fig. 10), the compressive residual stress caused by indentation, and the volume expansion of indentation-stress induced martensite in the untempered specimens. In any case, it is expected that after the final grinding procedure that erases the indents and most of the grain boundary cracks parallel to the surface, martensite plate cracks will remain for further studies. As confirmed by Part 2 of this study, martensite plate cracks proved to be efficient tools for the generation of white-etching matter given their narrow width that allowed cracked surfaces to rub against each other and their ability to branch out to deflect

the contact-stress induced fractures. Instead, fatigue-induced grain boundary cracks grew to almost 2 mm in length in 2.8×10^8 cycles (551.2 h) suggesting their poor applicability for such experiments due to the higher propensity to lead to macroscopic failure of the specimen [7].

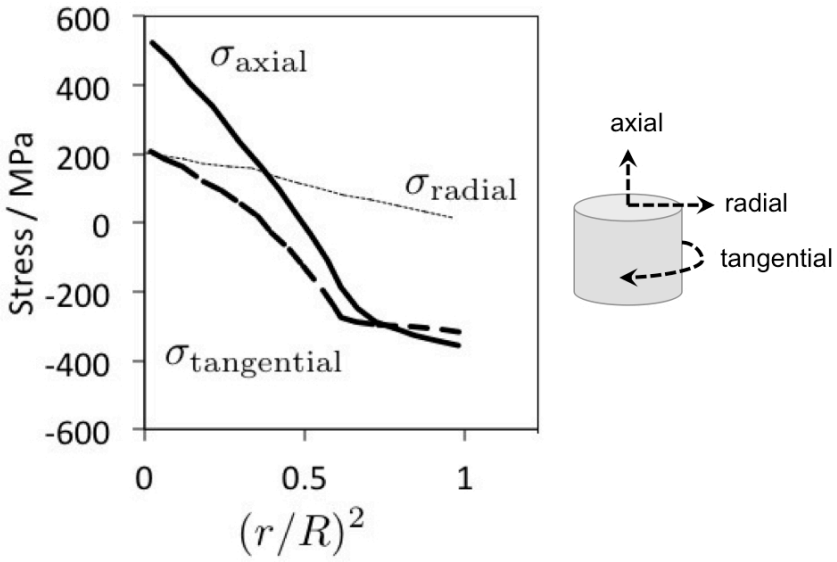

Figure 10: Residual stress on quenching a steel cylinder in water at 273 K (0 °C) from 873 K (600 °C), adapted from [25].

The flow chart of fig. 11 summarises the pathways to different crack morphologies. In addition, fig. 12 schematically depicts the heat treatments necessary for such cracks to be created.

4. Conclusions

- The optimum treatment to produce a sparse dispersion of martensite plate microcracks in a 10 mm diameter sample requires austenitisation at 1153 K (880 °C) for 10 min followed by quenching in oil at room temperature. Alternatively, if fine grain boundary cracks are desired for the same sample size, austenitisation at 1173 K (900 °C) for 10 min and quenching in oil at room temperature is the heat treatment required.

- The best treatment to create many martensite plate cracks in a rod 10 mm in diameter requires austenitisation at 1313 K (1040 °C) for 90 min, followed by cooling in air for approximately 50 s, and quenching in oil at room temperature.

- Surface cracks can be introduced reliably by indenting with a Vickers diamond and a 130 kg load for samples harder than ~750 HV30.

- Indentation cracks can be widened via isostatic pressure or propagated through bending if the sample geometry permits.

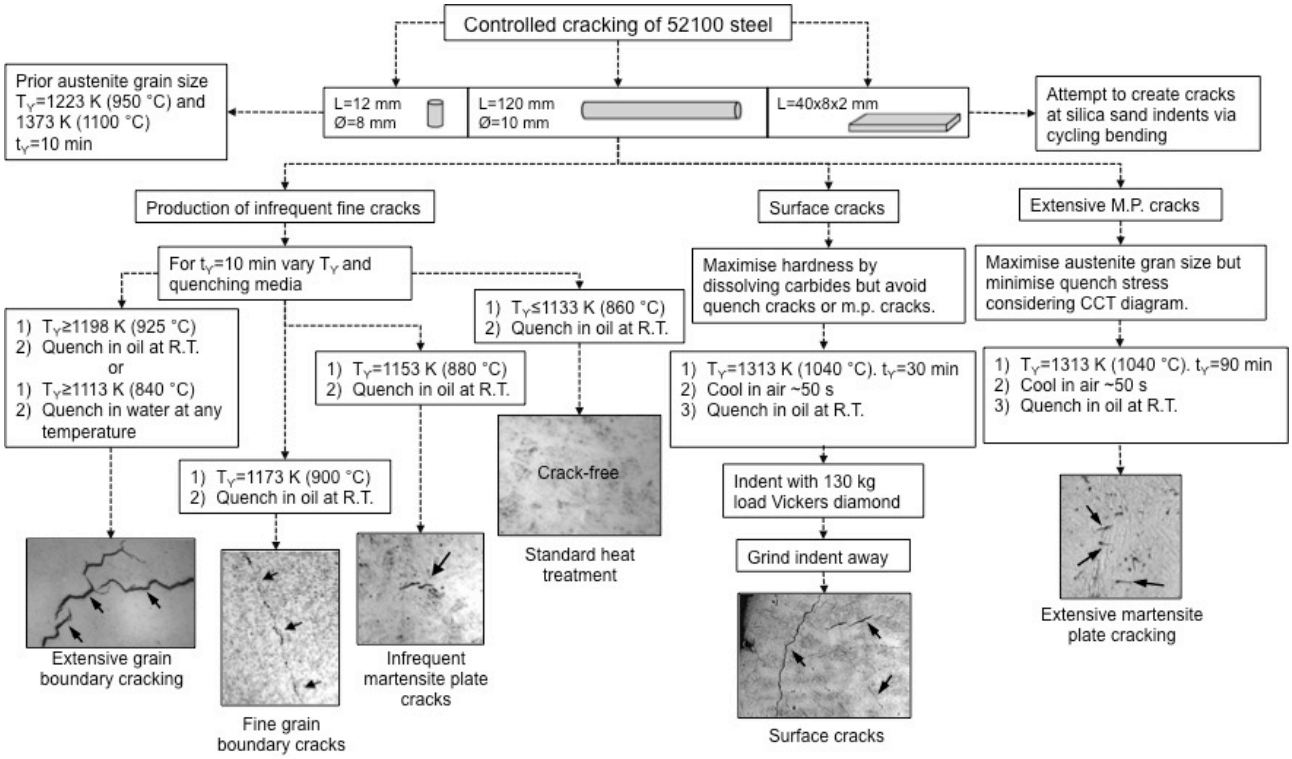

Figure 11: Flow chart of experimental work, where m.p. stands for martensite plate cracks, R.T. for room temperature, and CCT for continuous cooling transformation.

- The generation of additional martensite by cryogenic treatment in liquid nitrogen increases the frequency (though not the depth) of surface cracks during indentation. The Vickers diamond indentation load required is 130 kg because this permits the subsequent removal of the surface to a depth of 250 μm without grinding away the cracks.

- The most successful surface cracking treatment for a 10 mm in diameter sample, consists of austenitising at 1313 K (1040 °C) for 30 min, cooling in air for approximately 50 s and quenching in oil at room temperature. The sample should be then indented with a Vickers hardness tip and a 130 kg load. Finally, 120 μm of the surface material have to be ground away to eliminate completely the indent whilst the surface and subsurface cracks created upon indentation remain. For the study of real bearings, grinding away 250 μm is recommended.

5. Acknowledgements

We are thankful to Dr Steve Ooi for advice on experimental techniques and Dr Carsten Schwandt for the use of the vacuum oven and isostatic press. W. Solano-Alvarez is thankful to CONACyT, the Cambridge Overseas Trusts, and the Roberto Rocca Education Program for financial support.

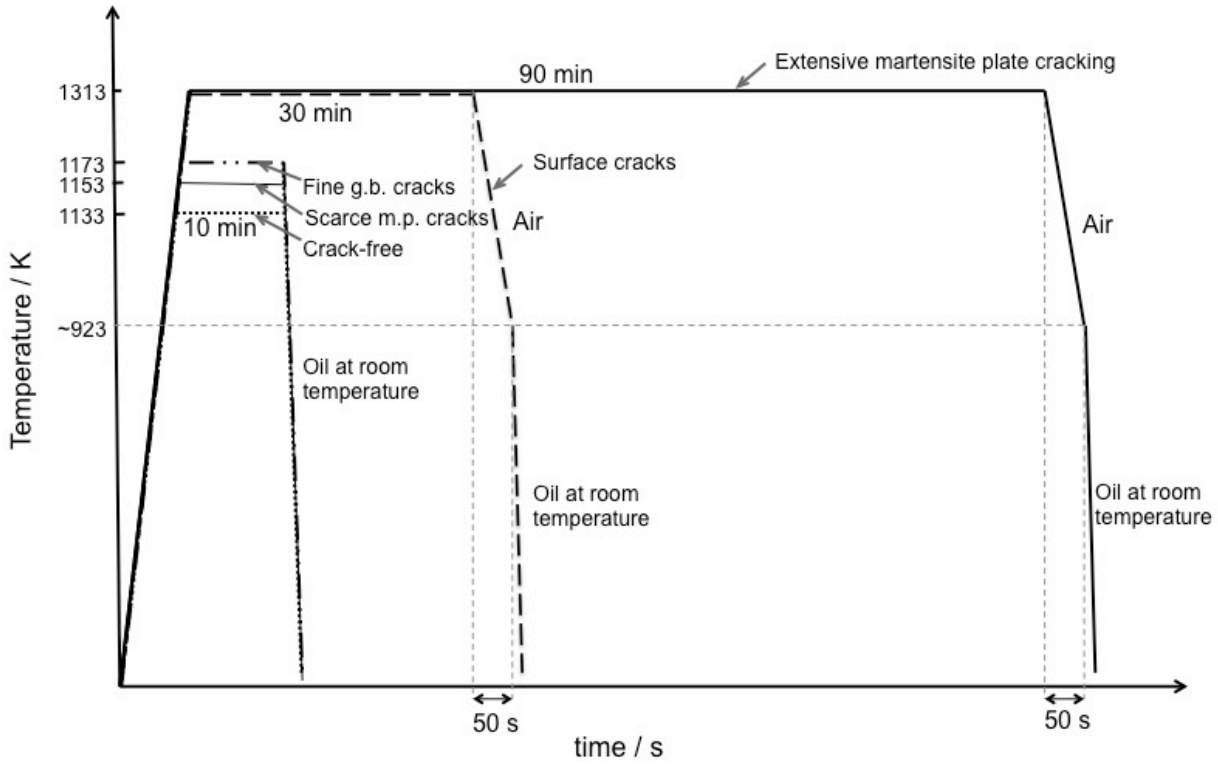

Figure 12: Schematic of final heat treatments for a 10 mm in diameter and 120 mm long rod, where m.p. stands for martensite plate and g.b. for grain boundary cracks. The surface cracked sample was indented after the depicted heat treatment.

6. References

[1] R. Errichello, S. Sheng, J. Keller, A. Greco: Wind turbine tribology seminar: Tech. Rep. DOE/GO-102012-3496 February 2012: U. S. Department of Energy: Golden, Colorado, USA 2012.

[2] A. Grabulov, U. Ziese, H. W. Zandbergen: Scripta Materialia 2007, vol. 57, pp. 635–638.

[3] M.-H. Evans: Materials Science and Technology 2012, vol. 28, pp. 3–22.

[4] H. K. D. H. Bhadeshia: Progress in Materials Science 2012, vol. 57, pp. 268–435.

[5] K. Hiraoka, M. Nagao, T. Isomoto: Journal of ASTM International 2007, vol. 3, pp. 234–240.

[6] R. Fougères, G. Lromand, A. Vincent, D. Nelias, G. Dudragne, D. Girodin, G. Baudry, P. Daguier: A new physically based model for predicting the fatigue life distribution of rolling bearings in: J. M. Beswick (Ed.), Bearing Steel Technology: ASTM International, Philadelphia, USA, 2002: pp. 197–212.

[7] W. Solano-Alvarez, H. K. D. H. Bhadeshia: Submitted to Metallurgical and Materials Transactions A 2013.

[8] R. G. Davies, C. L. Magee: Metallurgical Transactions 1972, vol. 3, pp. 307–313.

[9] A. R. Marder, A. O. Benscoter: Metallurgical & Materials Transactions B 1970, vol. 1, pp. 3234–3237.

[10] A. R. Marder, A. O. Benscoter, G. Krauss: Metallurgical Transactions 1970, vol. 1, pp. 1545–1549.

[11] J. Lyman: Journal of Engineering Materials and Technology 1984, vol. 106, pp. 253–256.

[12] S. Chatterjee, H. K. D. H. Bhadeshia: Materials Science and Technology 2006, vol. 22, pp. 645–649.

[13] M. G. Mendiratta, J. Sasser, G. Krauss: Metallurgical Transactions 1972, vol. 3, pp. 351–353.

[14] J. M. Beswick: Steel with a composition of iron, carbon, phosphorus and molybdenum: Tech. Rep. US Patent 4,961,904: U. S. Patent Office 1990.

[15] Z. Lei, A. Zhao, J. Xie, C. Sun, Y. Hong: Theoretical and Applied Mechanics Letters 2012, vol. 2, pp. 031003.

[16] W. Solano-Alvarez, E. J. Song, D. K. Han, D.-W. Suh, H. K. D. H. Bhadeshia: Submitted 2014.

[17] B. Chalmers, R. King, R. Shuttleworth: Proceedings of the Royal Society A 1948, vol. 193, pp. 465–483.

[18] K. Ryttberg, M. K. Wedel, V. Recina, P. Dahlman, L. Nyborg: Materials Science & Engineering A 2010, vol. 527, pp. 2431–2436.

[19] L. Karmazin: Materials Science & Engineering A 1991, vol. 142, pp. 71–77.

[20] H. Brandis: Vergleichende untersuchungen an DEW–100 Cr 6 und zwei niedriglegierten wälzlagerstählen amerikanischer entwicklung: Tech. Rep. 227/72: Deutsche Edelstalwerke Aktiengesellschaft Krefeld Forschungsinstitut: Germany 1972.

[21] I. L. Goldblatt: Tribology Transactions 1973, vol. 16, pp. 150–159.

[22] N. A. Branch, N. K. Arakere, V. Svensdsen, N. H. Forster: Journal of ASTM International 2010, vol. 7, pp. ID JAI102529 1–18.

[23] A. Yonezu, T. Hara, T. Kondo, H. Hirakata, K. Minoshima: Materials Science and Engineering A 2012, vol. 531, pp. 147–154.

[24] C. A. Stickels: Metallurgical Transactions 1974, vol. 5, pp. 865–874.

[25] B. Hildenwall: Prediction of the residual stresses created during quenching: Ph.D. thesis: Linkoping University: Sweden 1979.